Geomechanics and Engineering, *Vol. 18, No. 5 (2019) 503-513*
DOI: https://doi.org/10.12989/gae.2019.18.5.503

Investigation of the liquefaction potential of fiber-reinforced sand

Yetis Bulent Sonmezer*

Department of Civil Engineering, Faculty of Engineering, Kirikkale University, 71450 Kirikkale, Turkey

(Received April 28, 2019, Revised July 2, 2019, Accepted July 18, 2019)

Abstract. In the present, the liquefaction potential of fiber-reinforced sandy soils was investigated through the energy-based approach by conducting a series of strain-controlled cyclic simple shear tests. In the tests, the effects of the fiber properties, such as the fiber content, fiber length, relative density and effective stress, and the test parameters on sandy soil improvement were investigated. The results indicated that the fiber inclusion yields to higher cumulative liquefaction energy values compared to the unreinforced (plain) ground by increasing the number of cycles and shear strength needed for the liquefaction of the soil. This result reveals that the fiber inclusion increases the resistance of the soil to liquefaction. However, the increase in the fiber content was determined to be more effective on the test results compared to the fiber length. Furthermore, the increase in the relative density of the soil increases the efficiency of the fibers on soil strengthening.

Keywords: earthquake, fiber, liquefaction, reinforced soil, sand, cyclic simple shear test, energy-based model

1. Introduction

During an earthquake, the excess pore water pressure increases tremendously and the effective stress decreases in the loose sand layers saturated with water due to the cyclic shear stresses, caused by the shear waves. As a result of this, the saturated loose sandy soil layer loses its strength and induces significant damage to the engineering structures on the ground (Towhata 2008). The typical examples of this phenomenon, denoted as the soil liquefaction, were encountered in the Niigata and Alaska 1964, Loma Prieta 1989, Kobe 1995 and Chi-Chi 1999 earthquakes. On May 20th, 2012 (ML = 5.9) and May 29th, 2012 (ML = 5.8 and ML = 5.3), 27 people died and 12000 buildings were severely damaged during the earthquakes in Italy's Emilia Romagna Region. Significant and widespread liquefaction effects were observed in this earthquake, causing damage to buildings and infrastructure systems (Fioravante *et al.* 2012). Researchers focused their attention on this very phenomenon in the last few decades in order to understand the mechanism of the liquefaction and to reduce the damage caused by this kind of enormous calamities (Alavi and Gandomi 2012, Monkul *et al.* 2015, Baziar and Jafarian 2007).

The soil reinforcement procedures to reduce the soil liquefaction risk are reliable and efficient methods in the geotechnical earthquake engineering, adopted since the ancient times (Vercueil *et al.* 1997, Goktepe *et al.* 2008, Noorzad and Amini 2014). Researchers investigated the soil strengthening techniques by means of quantitative and analytical approaches. For this purpose, methods including the application of lime or fly ash, injection of cement or addition of geotextile to the soil were adopted till now (Krishnaswamy and Isaac 1995, Noorzad and Omidvar 2010, Diambra *et al.* 2010, Lovisa *et al.* 2010, Komak *et al.* 2015, Keramatikerman *et al.* 2017). The applied materials improve certain features of the soil, like the shear strength, compressibility, density, and hydraulic conductivity (Orakoglu *et al.* 2017, Jones 1999).

The previous studies indicated that the fiber use for soil strengthening improves the tensile strength of the soil (Ghazavi and Roustaei 2010, Zaimoglu 2010, Tang *et al.* 2016, Gullu and Khudir 2014). On the other hand, the studies on the liquefaction potential of fiber-reinforced soil indicated that the soil liquefaction is affected by the fiber length, fiber content and the surrounding pressure (Krishnaswamy and Isaac 1994, Ibraim *et al.* 2010, Maheshwari *et al.* 2012, Ashmawy and Bourrdeau 1998).

When compared to the stress- and strain-based approaches, the major advantages of the energy-based approach in liquefaction analysis are as follows. First, energy is a scalar quantity taking the entire spectrum of the ground motion into account (Baziar *et al.* 2011, Baziar and Jafarian 2007). Secondly, the use of the energy approach enables the inclusion of the strain, stress and material properties to the analysis (Liang 1995, Law 1990). The energy-based approach in the liquefaction evaluation was proposed by Nemat-Nasser and Shokooh (1979) as an alternative to the stress-based approach. This method mainly incorporates the fundamental components of the stress- and deformation-based approaches into the formulation. In a typical laboratory test, the shear stress, shear deformation and excess pore water pressure data can be recorded. The hysteresis loop can be produced from these shear stress and shear deformation data during the test. A typical loop, obtained from a deformation-controlled cyclic simple shear test, is illustrated in Fig. 1. The deformation energy in each loading cycle is equal to the area inside this hysteresis loop (Ostadan *et al.* 1996). In

*Corresponding author, Assistant Professor
E-mail: bsonmezer@kku.edu.tr

ISSN: 2005-307X (Print), 2092-6219 (Online)

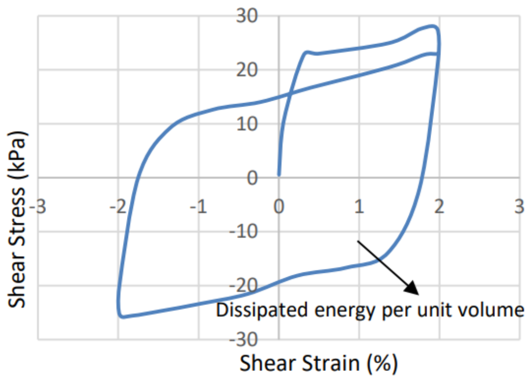

Fig. 1 Typical hysteresis loop under cyclic simple shear (Sonmezer 2019)

other words, this area represents the dissipated energy per unit volume of the ground mass (Green 2001). This situation is based on the idea that a portion of the energy during the ground deformation under dynamic loading is spread to the ground (Nemat-Nasser and Shokooh 1979). The instantaneous energy and the sum of this energy for the time intervals can be calculated from the dynamic test data up to the onset of liquefaction. The sum of this calculated energy is used as a measure of the energy capacity of the soil mass against liquefaction. The use of the capacity energy to assess liquefaction is rather appropriate because it depends on the shear stress and shear deformation induced during cyclic loading (Amini and Noorzad 2018).

Several energy-based methods have been proposed to assess the liquefaction potential of the soil over the last few decades (Simcock *et al.* 1983, Davis and Berrill 2001, Jafarian *et al.* 2012, Liang 1995, Law 1990). In these experimental studies, the total dissipated energy per unit volume of the soil was shown to be directly related to the excess pore water pressure, generated during undrained loading. Simcock *et al.* (1983) conducted a series of energy-based undrained dynamic triaxial tests. The results showed that more energy is distributed in the sample with an increase in excess pore water pressure. Towhata and Ishihara (1985) conducted a series of undrained tests using the Toyoura sand in the hollow cylindrical torsional shear test. Their results showed a strong relationship between the unit energy and the excess pore water pressure. In addition to laboratory tests, analysis methods based on field tests are also used to evaluate soil liquefaction. Cavallaro *et al.* (2018) analyzed soil liquefaction using the results of the Seismic and Dilatometer Marchetti Tests (SDMT) tests and soil properties obtained by field and laboratory tests and analyzed new tentative CRR-Kd correlations based on SDMT. They reported that the results obtained were consistent with other studies conducted in the same field.

The method of using fiber to strengthen the sandy soil has attracted a great deal of attention from researchers due to its features and advantages, such as its reliability, slow biodegradability and low cost (Hejazi *et al.* 2012). In particular, depending on their high tensile strength values that improve the soil strength, there has been an increasing interest on the fiber soil strengthening in recent years. However, fiber strengthening of the soil is still a relatively new technique and the ground-fiber performance mechanism needs to be fully investigated in every geotechnical project.

Sharma and Kumar (2017) reported that the strength and bearing capacity of the fiber-reinforced soil increased considerably with an increase in the relative density. Moreover, the previous researchers reported that the fibers can increase the ductility and liquefaction resistance of the soil (Park 2011, Ye *et al.* 2017). Some studies on this subject are summarized below.

Krishnaswamy and Isaac (1994, 1995) conducted a series of stress-controlled dynamic triaxial tests to investigate the effects of coir, woven and nonwoven geotextile reinforcing elements on the liquefaction resistance of the sandy soil. The results showed that the application of such reinforcement increased the liquefaction resistance of sandy soil samples. They also found that although the effect of the size of the test specimen was negligible, the parameters such as the effective confining pressure, stress ratio and interface friction of reinforcement have a significant effect on the liquefaction potential of the reinforced soil.

Chen and Loehr (2008) examined the behavior of fiber-reinforced and plain soil in the three-axial experimental setup under experimental conditions with and without drainage. They determined that the soil strengths of the fiber-reinforced specimens under drained experimental conditions exceeds the respective values of the same specimens under undrained experimental conditions at low deformation levels. The experiments conducted by Sadek *et al.* (2010) showed that a 0.5 to 1.5 % fiber content in the soil increases the shear strength values of the specimens. The studies carried out by Erken *et al.* (2015) showed that the dynamic strength values of sand specimens saturated to water increase with increasing fiber ratio.

Amini and Noorzad (2018) conducted a series of dynamic triaxial tests to investigate the liquefaction properties of Babolsar sand reinforced with randomly distributed fibers, using an energy-based approach. The effects of fiber content, fiber length, confining pressure and relative density were investigated. The results exhibited that the addition of fibers resulted in a higher cumulative energy by increasing the number of cycles required for liquefaction. In addition, comparative studies (Amini and Noorzad 2018, Kokusho 2013) have shown that the energy-based method is a good way to assess the liquefaction potential of fiber-reinforced sands.

Chegenizadeh *et al.* (2018) investigated the effect of fiber on the liquefaction resistance of low-plasticity silt by performing a series of dynamic triaxial tests on fiber-reinforced (BCF) and unreinforced samples. The results showed that increasing the BCF content and length increases the liquefaction resistance of the samples, whereas with an increase in the relative density (Dr), the liquefaction resistance of the reinforced sample becomes more pronounced than that of the unreinforced (plain) sample.

Although the previous studies, with the exception of a few ones, focused on the strength and deformation properties of the fiber-reinforced soil under static loading, the efficiency of the fibers, added by dispersing randomly, in improving the liquefaction potential of the sandy soil was revealed with the help of a series of cyclic simple shear tests in the present study. The aim of the present study was to investigate the liquefaction potential of the sandy soil, reinforced with propobilene fiber at a percentage of 0.25-1.00 %, using the strain-controlled cyclic simple shear test and an energy-based approach. The study also aimed at proposing a relationship for the cumulative liquefaction energy of the fiber-reinforced soil as a function of the fiber length, fiber content and effective stress.

2. Material and method

2.1 Material

The experiments, conducted within the present study, were realized using the clean beach sand from the Gallipoli beach, located on the shores of the Marmara Sea in Turkey. The physical properties of the sand are given in Table 1 and the grain size distribution graph is illustrated in Fig. 2. 6, 12 and 19 mm long monofilament polypropylene fiber were used for strengthening the soil. The manufacturer reported that the adopted fibers have a diameter of 0.031 mm, a specific density of 0.9, a tensile strength of 400 MPa and a modulus of elasticity value in the order of 1000-2500 MPa. The fibers and fiber-sand mixture used in the study are given in Fig. 3.

2.2 Specimen preparation

Moist tamping method was preferred in the preparation of samples. Ladd (1978) showed that this technique is good, acceptable and feasible. In addition, this technique prevents the segregation of the fibers as well as maintaining the uniformity of the reinforced samples (Wang *et al.* 2011). One of the advantages of this method is that it allows samples in a wide range of void ratio to be prepared (Ishihara 1993). Several published experimental studies indirectly assume that the fibers are oriented randomly throughout the soil mass. Such a random distribution and orientation will protect the soil strength isotropy and eventually prevent or delay the formation of localized deformation planes (Hejazi *et al.* 2012). However, the fibers were also reported to tend to be oriented horizontally in the preparation of the reinforced samples by moist tamping technique (Diambra 2007).

In the experiments, fibers at ratios of 0.25, 0.50 and 1.00 % by weight were used. When preparing fiber-reinforced samples, the required amount of dry sand was first mixed with unaired water at a ratio of about 5 % by weight of sand. The required amount of fiber was added to this mixture, mixed thoroughly in the electric mixer and this mixture was divided into five equal parts. Then, the sand-fiber mixture, prepared for the first layer, was placed and stabbed in the test mold with a height of 46 mm and a diameter of 100 mm. Next, the same procedure was followed for each layer and samples with a relative density of 30 % and 50 % were prepared.

2.3 Test procedure

Experiments performed within this study were realized by using the cyclic simple shear test. This device can accomplish one-, two- and three-dimensional (1D, 2D and 3D) loading. 1D and 2D loading is conducted with the help of the pistons on the right and left side of the device, while the 3D loading is done by means of the piston standing in an upright position on the device and this piston has a force capacity of 10 kN. The device can apply either sinusoidal loading or a random loading, formed by entering the displacement record of a ground motion. The device used in the study is depicted in Fig. 4.

Mostly, specimens with a relative density of 30 % were tested, since the main purpose of this study was to observe the effect of fiber strengthening in loose sand layers saturated with water and with high liquefaction potential

Table 1 Properties of sand used in experiments

Property	Value
USCS classification symbol	SP
Median grain size, D50 (mm)	0.33
Specific gravity, Gs	2.63
Max. void ratio (emax)	0.90
Min. void ratio (emin)	0.62
Cu	1,52
Cc	1,04

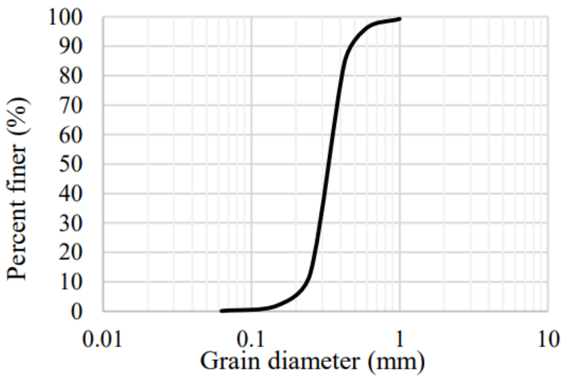

Fig. 2 Grain distribution curve of sand used in experiments

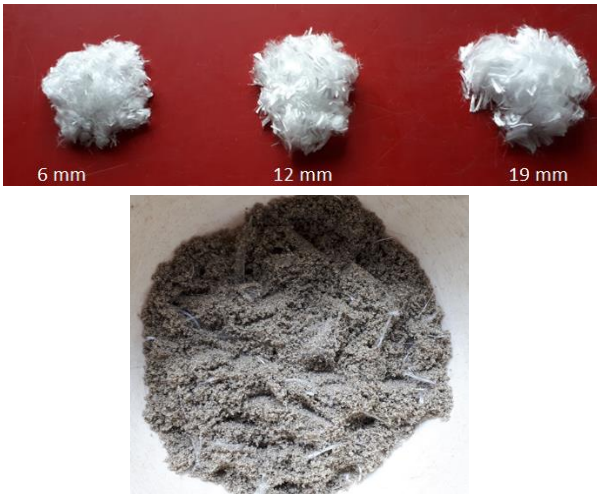

Fig. 3 The fibers and fiber-sand mixture used in the study

Fig. 4 The cyclic simple shear test setup used in the experiments

Table 2 Test results

Test No	$\sigma'v$(kPa)	F_C (%)	F_L (mm)	D_r (%)	W(J/m^3)
1	25	0		30	791
2	50	0		30	1463
3	100	0		30	2427
4	25	0.25	6	30	1282
5	50	0.25	6	30	1833
6	100	0.25	6	30	3268
7	25	0.5	6	30	3881
8	50	0.5	6	30	5027
9	100	0.5	6	30	5500
10	25	1	6	30	4760
11	50	1	6	30	6484
12	100	1	6	30	6997
13	25	0.25	12	30	1561
14	50	0.25	12	30	2692
15	100	0.25	12	30	5763
16	25	0.5	12	30	4574
17	50	0.5	12	30	5114
18	100	0.5	12	30	6489
19	25	1	12	30	4933
20	50	1	12	30	7112
21	100	1	12	30	10979
22	25	0.25	19	30	2797
23	50	0.25	19	30	4289
24	100	0.25	19	30	6757
25	25	0.5	19	30	4591
26	50	0.5	19	30	7167
27	100	0.5	19	30	11507
28	25	1	19	30	5784
29	50	1	19	30	9669
30	100	1	19	30	18509
31	50	0		50	2645
32	50	0.25	12	50	4120
33	50	0.5	6	50	12607
34	50	0.5	12	50	13313
35	50	0.5	19	50	13658
36	50	1	6	50	26465
37	50	1	12	50	31010
38	50	1	19	50	45589

Table 2 Continued

where effective stress (kPa), FC: fiber content in percent (%), FL: fiber length (mm), Dr: Relative density (%) W: Cumulative liquefaction energy (J/m^3)

during an earthquake. However, in order to see the effect of relative density on fiber strengthening, few specimens with 50 % relative density were also tested. In order to ensure that the specimens were saturated with water and to prevent air bubbles from remaining in the sample, CO2 was applied for 20 min. to the samples from bottom towards top. After flushing with CO2, the deaired water was given to the sample from bottom to top from the water deairing apparatus under low pressure to assure full saturation of the sample to water. Airless water with a volume of at least 5 times the sample volume was passed through the sample. After the saturation process was completed, the effective stress was applied to the sample and the sample was anisotropically consolidated under this stress.

During cyclic loading, a uniform sinusoidal shear strain with a frequency of 0.1 Hz was applied in the horizontal direction, which is recommended for this type of test equipment Chen and Loehr (2008) although being less than a typical earthquake frequency. This stress develops with the help of the horizontal movement of the red plate below the sample mold, shown in Fig. 4. Excessive pore water pressures developed during the tests were measured by sensitive pressure sensors, located above and below the sample. All parameters during the experiment were automatically recorded by the software of the cyclic simple shear test apparatus to the experiment file, as 20 readings for each cycle. In the experiments, the samples were assumed to liquefy as soon as an excess pore water pressure equal to the initial effective vertical stress develops. In the study, 38 deformation-controlled cyclic simple shear tests were performed under 3 % deformation and undrained conditions and for the effective stress values of 25, 50 and 100 kPa. In some studies, it has been shown that the liquefaction energy of the soil under dynamic loading is little or not dependant on shear strain amplitude (Figuera *et al.* 1994, Liang 1995). Furthermore, in stress-controlled dynamic tests, it is assumed that the tested sample is liquefied when either the excess pore pressure is equal to the effective stress or when the shear strain amplitude reaches the double amplitude 6% or 10% (DeAlba et al 1976, Ishara 1985). Therefore, in this study, the double amplitude 6% (unidirectional 3%) deformation level tests were performed. The experiments yielded to the cumulative energy values of fiber-reinforced sand samples up to the onset of liquefaction. The expression given in Equation 1 is frequently used in the literature to calculate the cumulative liquefaction energy per unit volume. This expression was also used in this study. (Figueroa *et al.* 1994, Liang 1995).

$$W = \frac{1}{2}\sum_{i=1}^{n}(\tau_n + \tau_{n+1})(\gamma_{n+1} - \gamma_n) \qquad (1)$$

where W: Cumulative total energy, τ: shear stress, γ: shear unit deformation and n: number of cycles recorded to liquefaction. The dissipate energy for each cycle from the first cycle to the cycle n, in which liquefaction occurs, is calculated using the above formula and these energies are summed to determine the total liquefaction energy (J/m3) of the sample. The cumulative energy results and initial test conditions of all tests performed in this study are given in Table 2.

3. Results and discussion

In this section, the number of cycles, excess pore water pressure ratio, shear modulus ratio of the fiber-reinforced and unreinforced samples and the relationship of these parameters with the cumulative liquefaction energy are shown. In addition, the effect of fiber properties (fiber content and fiber length) and test parameters (effective stress, relative density) on the liquefaction resistance were presented and discussed. The results of the typical experiment of a sample under 50 kPa effective stress, with a 30 % relative density and 0.25 % fiber content and reinforced with 6 mm long fibers, are shown in Figures 5-9. The hysteresis loop showing the change of the shear stress with the shear deformation is shown in Figure 5. As can be seen from the figure, the area under the curve decreases with increasing number of cycles. The reason for this reduction is the increase in excess pore water pressure. At the moment of liquefaction, on the other hand, the area under the loop reduces to a major extent and the loop takes a nearly straight form. In this experiment, the variation of the 3 % shear strain, applied to the sample, with number of cycles is given in Fig. 6. In deformation-controlled

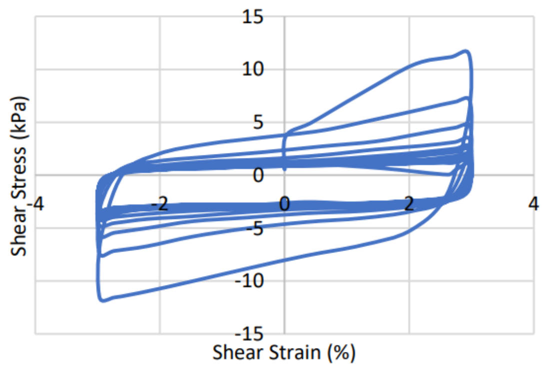

Fig. 5 The hysteresis loop

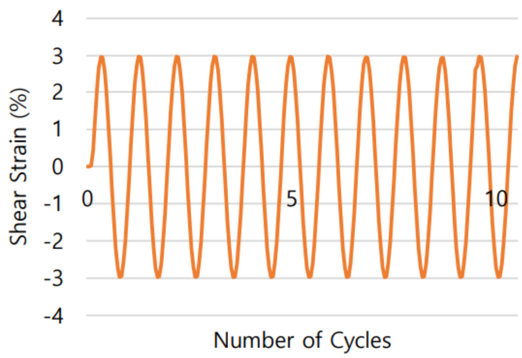

Fig. 6 Cyclic shear strain variation with the number of cycles

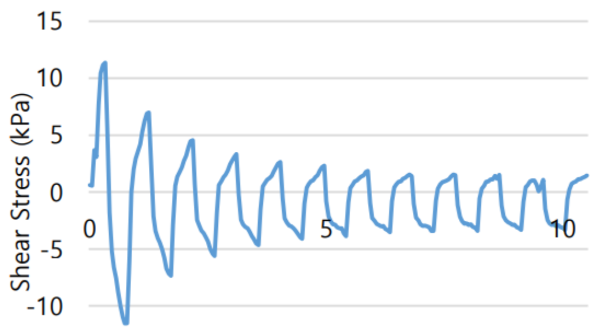

Fig. 7 Cyclic shear stress variation with the number of cycles

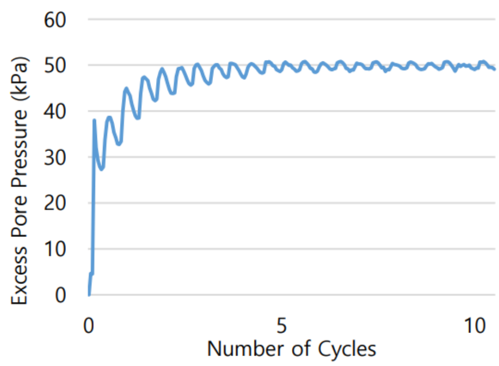

Fig. 8 Variation of the excess pore pressure with the number of cycles

experiments, the amplitude of the shear strain is kept constant from the beginning of the experiment to the end.

Due to the applied shear deformation, the excess pore water pressure in the sample increases until it is equal to vertical effective stress.

Fig. 7 shows the variation of the shear stress of the aforementioned test with the number of cycles. Due to the shear strain, applied in a controlled manner, the shear stress decreases as approaching liquefaction as a result of the reduction in the soil resistance and eventually reaches a constant value. Theoretically, the shear stress does not become exactly zero as in a liquid. This situation is thought to stem from the friction existing in the test system. Fig. 8 shows the change in the excess pore water pressure with the number of cycles. Excess pore water pressure, which is one of the most important indicators of soil liquefaction, increases rapidly until it is equal to vertical effective stress due to increased sample deformation and settling of sand grains more tightly and it continues horizontally with the occurrence of liquefaction.

3.1 The relationship between the cumulative dissipated energy and the number of cycles

The change in the dissipated energy per unit volume with the fiber content and fiber length is given in Figs. 9 and 10, respectively. As can be seen from the figures, the cumulative dissipated energy increases with increasing number of cycles until reaching liquefaction depending on the increase in the fiber content as well as the fiber length. Especially when compared to the plain samples, the liquefaction resistance of the reinforced samples can be seen to increase to a considerable extent with an increase in the fiber content and length. This increase is thought to originate from the increase in the shear strength of the soil sample due to the presence of fibers. This shows that the fibers mixed with the sand have a clearly significant effect on the susceptibility of the sandy soil to liquefaction.

3.2 The dissipated energy and excess pore water pressure relationship

Excess pore water pressure ratio (r_u) is defined as the ratio of the excess pore water pressure to effective stress. When ru = 1, the soil loses its strength and liqufies. Figure 11 shows the relationship between excess pore water pressure ratio and the cumulative dissipated energy with increasing fiber length. To clarify, the dissipated energy and the number of cycles required to reach liquefaction increases in the presence of fibers in the soil. The reason for this increase is thought to be the difficulty in settling of the grains, caused by the increase in the fiber length, during the re-settling of the sand grains with increasing deformations in the test. This can be also explained by the fact that polypropylene fibers are mobilized under increasing deformations since they constitute an extensible reinforcing material and their tensile strength is high (Amini and Noorzad 2018).

In Fig. 12, the relationship between the excess pore water pressure and the cumulative dissipated energy is shown for varying fiber content. As for increasing fiber length, the amount of dissipated energy per unit volume up to the onset of liquefaction increases with increasing fiber

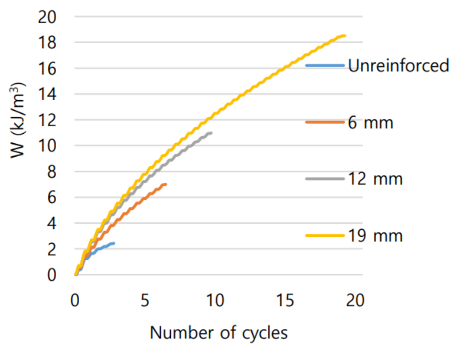

Fig. 9 The fiber length changes in the presence of 100 kPa effective stress, 1% fiber content and 30% relative density

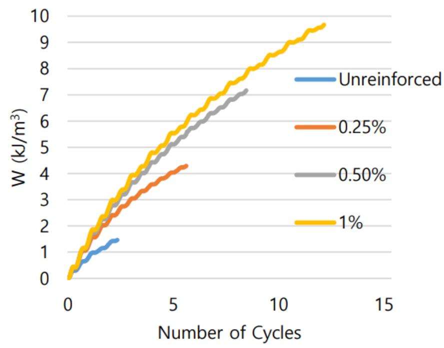

Fig. 10 The fiber content changes in the presence of 50 kPa effective stress, 30% relative density and 19 mm long fibers

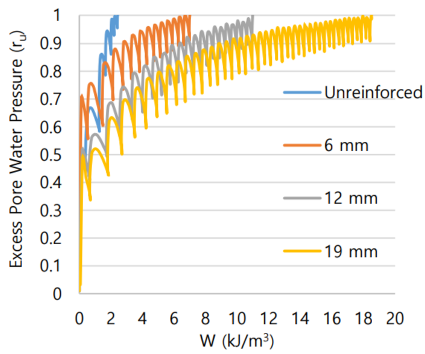

Fig. 11 The cumulative dissipated energy change for varying fiber length in the presence of 100 kPa effective stress, 30% relative density and 1% fiber content

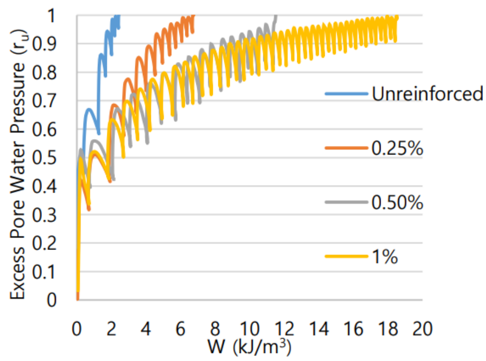

Fig. 12 The cumulative dissipated energy change for varying fiber content in the presence of 100 kPa effective stress, 30% relative density and 19 mm fiber length

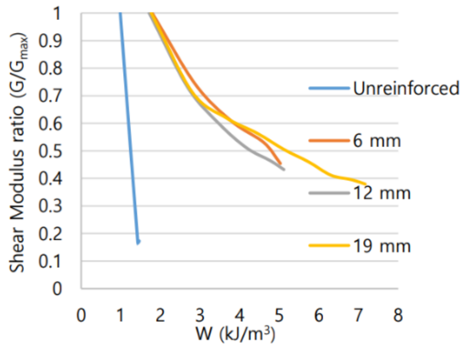

Fig. 13 The relationsip between the shear modulus ratio and unit energy for 50 kPa effective stress and 0.5% fiber content

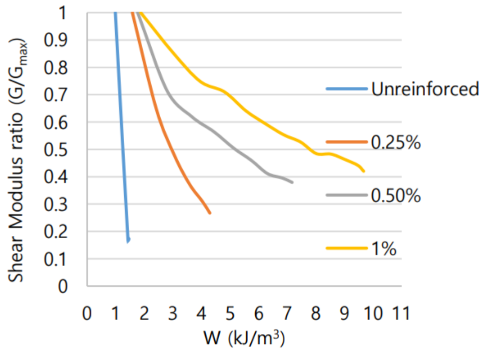

Fig. 14 The relationsip between the shear modulus ratio and unit energy for 50 kPa effective stress and 19 mm fiber length

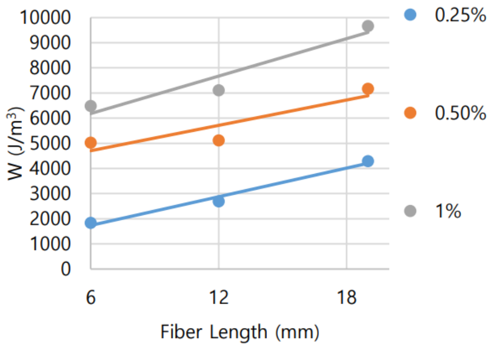

Fig. 15 The relationship between the cumulative liquefaction energy and fiber length for different fiber contents, 50 kPa effective stress and 30% relative density

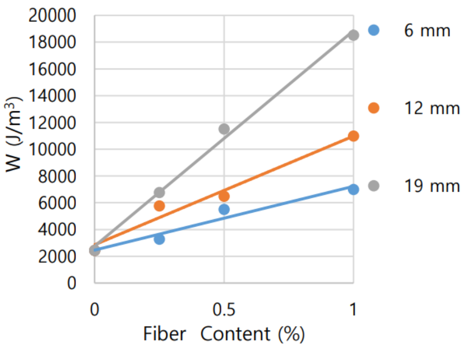

Fig. 16 The relationship between the cumulative liquefaction energy and fiber content for different fiber lengths, 100 kPa effective stress and 30% relative density

content. That is, by mixing fibers to the sand, the reduction of the soil shear strength is significantly delayed and its resistance to liquefaction increases.

3.3 Relationship between the dissipated energy and the shear modulus

Shear modulus is an important parameter for evaluating the dynamic properties of soils. The shear modulus ratio (G / Gmax) is defined as the ratio of the shear modulus (G) in the cycle in which the liquefaction occurs to the maximum shear modulus (Gmax) (Kokusho 2013). Fig. 13 shows the relationship between the cumulative dissipated energy and shear modulus ratio for different fiber lengths in the presence of 50 kPa effective stress, 30% relative density and 0.5% fiber ratio. Until the initiation of liquefaction, the shear modulus rapidly decreases with increasing unit energy in the non- reinforced sample, while the shear modulus ratio reduction is much more gradual with increasing unit energy in the reinforced sample. This finding can be explained by the long-term preservation of the soil hardness and the increased resistance to liquefaction in the presence of fibers. However, the unit energy and shear modulus ratio is not affected significantly by the increase in fiber length.

Fig. 14 shows the relationship between the unit energy and shear modulus for different fiber ratios in the presence of 50 kPa effective stress, 30% relative density and 19 mm fiber length. As expected, the samples reinforced with fibers yield to higher unit energy values compared to the unreinforced ones. The addition of fibers causes better interlocking of the soil particles. In the reinforced samples, the shear modulus ratio decreases very slowly with increasing unit energy and the sample exhibits a much slower stiffness degradation. In addition, as the fiber ratio increases, this situation becomes more pronounced and the relationship is not linear. The increase in the soil liquefaction resistance with the addition of fibers was also stated in other previous studies (Amini and Noorzad 2018, Chegenizadeh *et al.* 2018).

3.4 Effects of the fiber content and fiber length

Some other studies have shown that the energy-based approach is a good index for assessing liquefaction (Baziar and Jafarian 2007, Figueroa *et al.* 1994). Figs. 15 and 16 show the relationships between the cumulative liquefaction energy at the onset of liquefaction and the fiber length (FL) and fiber content (FC), respectively. Fig. 15 shows the relationship between the cumulative liquefaction energy and fiber length of samples with 50 kPa effective stress and 30% relative density for various fiber contents. As seen, the cumulative liquefaction energy increases linearly with the fiber length. The cumulative energy of the sample with 19 mm fiber length is 42% higher than the respective value of the sample with 6 mm fiber length for a fiber content of 0.50 %.

Fig. 16 shows the relationship between the cumulative liquefaction energy and fiber content of the samples with 100 kPa effective stress and 30% relative density for various fiber lengths. The cumulative energy increases by 90% when the ratio of the 12 mm long fibers, mixed

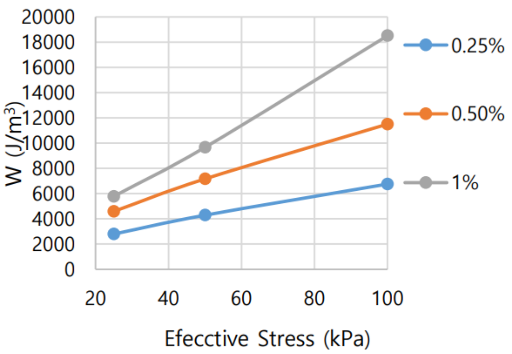

Fig. 17 The relationship between the effective stress and liquefaction energy for a relative density of 30%, a fiber length of 19 mm, but for different fiber contents

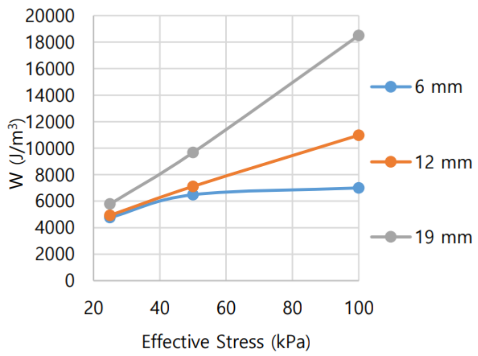

Fig. 18 The relationship between the effective stress and liquefaction energy for a relative density of 30%, a fiber ratio of 1 %, but for different fiber lengths

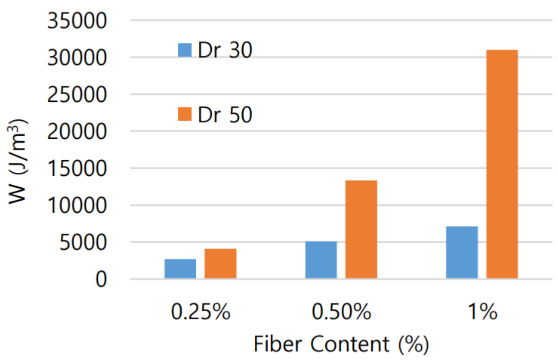

Fig. 19 Variation in the liquefaction energy with respect to the relative density and for an effective stress of 50 kPa and a fiber length of 12 mm

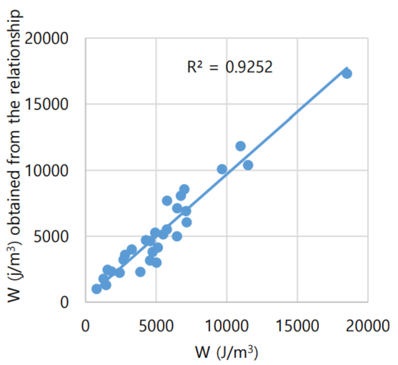

Fig. 20 Experimental results compared to the analytical estimates from the expression

randomly with the sand, increases from 0.25 % to 1.00 %. The amount of energy required to reach liquefaction can be clearly observed to increase regardless of the fiber content and fiber length when fibers are mixed randomly with the sand. However, as can be seen from the increase in the energy ratio values, the amount of energy required to reach liquefaction increases to a greater extent with an increase in the fiber content as compared to an increase in the fiber length. This shows that the increase in the fiber content is more effective than increasing the fiber length in preventing the liquefaction-induced strength loss of soil. Similar results were reported by Consoli *et al.* (2002) and Amini and Noorzad (2018).

3.5 Effects of the effective stress and relative density

Fig. 17 shows the variation of the liquefaction energies of the samples with different fiber ratios, 30% relative density and 19 mm fiber length with respect to the effective stress. Fig. 18, on the other hand, shows the variation of the liquefaction energy with respect to the effective stress for different fiber lengths, 1 % fiber ratio and 30% relative density. The energy required for liquefaction can be clearly seen to increase linearly with increasing effective stress in the cases of both fiber content and fiber length increase. In other words, the resistance of the sample to liquefaction increases if either the fiber content or the fiber length increases. For example, in the presence of 30% relative density and 19 mm fiber length, the liquefaction energy increases by 141% for a fiber content of 0.25% when the effective stress is increased from 25 kPa to 100 kPa. Under the same circumstances, but for a fiber ratio of 1%, the increase in the energy is 220%. Similarly, the increase in the liquefaction energy when increasing the effective stress from 25 kPa to 100 kPa is only 21% in the presence of 6 mm long fibers in the sandy soil, yet 164% in the presence of 19 mm long fibers. These results indicate that the liquefaction energy is strongly dependant on the effective stress and the increase in the fiber content is more influential on the liquefaction energy than the increase in the fiber length. These results are in agreement with the ones obtained by Jafarian *et al.* (2012) and Figuera *et al.* (1994).

Fig. 19 illustrates the effect of the relative density on the liquefaction energy for different fiber contents. As seen clearly, the relative density has a positive contribution to the liquefaction energy in all values of fiber content. With increasing relative density, the contribution of fiber strengthening becomes more pronounced. Namely, under an effective stress of 50 kPa and in the presence of 12 mm fibers, the increase in the liquefaction energy is 53% in the presence of 0.25% fiber content when the relative density is increased from 30% to 50%. Under the same circumstances, but a fiber content of 1% this time, the increase is about 336 %. This finding most probably originates from the increase in the contact between the sand particles at higher relative densities, and therefore, the higher resistance of the particles to rearrangement under dynamic loading. Normally, this situation results in an increase in the shear resistance, and thus, in the energy needed for liquefaction. In other words, the composite material exhibits

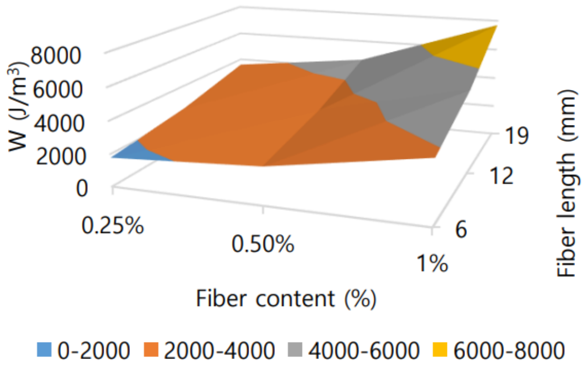

(a)

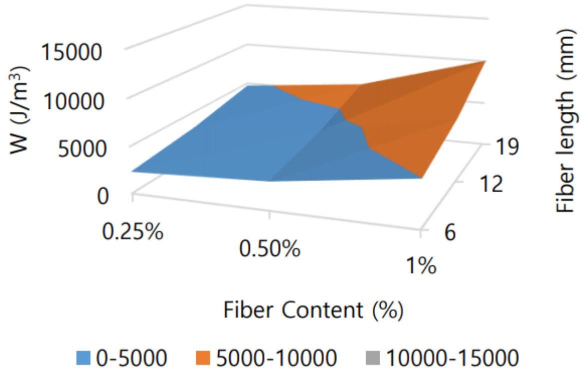

(b)

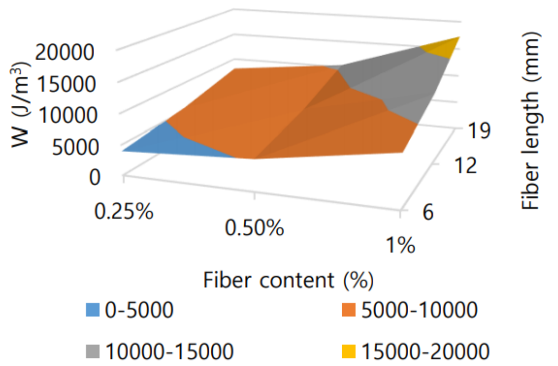

(c)

Fig. 21 The cumulative liquefaction energy variation with respect to the fiber length and fiber content (a) 25 kPa, (b) 50 kPa and (c)100 kPa

a higher resistance to the liquefaction when the density increases.

3.6 Regression analysis

In this section, a generalized equation was obtained by conducting a regression analysis using the effective stress, fiber content, fiber length and the cumulative dissipated liquefaction energy per unit volume (for 30 % relative density). In the analysis, the cumulative liquefaction energy per unit volume is the dependent variable, while the effective stress, fiber content and fiber length are the independent variables. The expression with the highest correlation coefficient (R^2=0.92) from the analysis is given in Eq. (2).

$$W\left(\frac{J}{m^3}\right) = \mathrm{Exp}(0.0108 \cdot \sigma_v' + 1.017 \cdot F_C + 0.054 \cdot F_L + 6.633) \tag{2}$$

$$R^2 = 0.92$$

where W is cumulative dissipate energy in J/m^3, σ_v' is the effective stress in kPa; F_C is the fiber content percentage (%); F_L is the fiber length in mm.

The standard errors for the regression coefficients are 0.00102, 0.09939 0.006029, 0.14529, respectively. The estimates from the expression (Equation 1) are illustrated in Fig. 20 together with the experimental liquefaction energy values. The experimental results are clearly in close agreement with the analytical estimates from the proposed equation.

In Fig. 21, the relationship between the liquefaction energy, calculated from Equation (1), and FC and FL was illustrated for various values of the effective stress. As observed in the experiments, the liquefaction energy, calculated from the expression developed from the regression analysis, can be observed to be strongly dependant on the fiber ratio and fiber length. Similar conclusions were drawn by Amini and Noorzad (2018).

4. Conclusions

A series of strain-controlled cyclic simple shear tests were conducted to evaluate the susceptibility of the sandy soils, which are originally susceptible to liquefaction, with the addition of randomly distributed fibers. For this purpose, the effects of parameters including the fiber content, fiber length, effective stress and relative density were investigated through the energy-based approach. The regression analysis on the test results yielded to an expression for estimating the liquefaction energy values of fiber-reinforced sands. The conclusion drawn from the present experimental and analytical studies are as follows:

- A significant increase in the cumulative liquefaction energy and the cycle number of the fiber-reinforced sandy soil was observed compared to the plain soil. That is, the fiber reinforcement has created limitations in the lateral movement of the sand used in the experiments and significantly increased its resistance to liquefaction.
- The presence of fibers strongly influences the development of the pore water pressure. In other words, the increase in excess pore water pressure is very slow in the presence of fibers. The same conclusion is valid for both the increase in fiber content and the increase in fiber length. This is thought to stem from the fact that the fiber increases the energy absorption capacity of the sand due to being an extensible material.
- Shear modulus is an important indicator for the stiffness degradation. When the reinforced and unreinforced samples are compared in terms of shear modulus, the shear modulus ratio in the unreinforced specimens can be seen to decrease rapidly with increasing unit energy. The decrease in the shear modulus ratio of the reinforced specimens was observed to be much slower with increasing unit energy. However, with the increase in fiber content, the reduction in the shear modulus ratio was observed to be much more

noticeable, while this reduction was much less smaller in the case of an increase in the fiber length.

• With the increase in the relative density, the resistance of the fiber-reinforced soil to liquefaction increases further. However, the effect of strengthening through increasing the fiber content is more pronounced in semi-stiff sands (50%) compared to loose sands (30%).

• With the increase in the effective stress, the liquefaction energy of the fiber-reinforced soil increases, and thus, the resistance of the soil to liquefaction increases. However, the increase in the fiber content is much more effective in increasing to resistance of the soil to liquefaction compared to increasing the fiber length.

• Through a regression analysis on the cyclic simple shear test results, an equation expressing the liquefaction energy of the sand as a function of the fiber content, fiber length and effective stress was proposed for a relative density of 30%.

Acknowledgments

Experiments were performed at the Soil Mechanics Laboratory of Ankara University. Thank you very much Dr. Kamil Kayabalı for his help.

References

Alavi, A.H. and Gandomi, A.H. (2012), "Energy-based numerical models for assessment of soil liquefaction", *Geosci. Front.*, **3**(4), 541-555. https://doi.org/10.1016/j.gsf.2011.12.008.

Amini, P.F. and Noorzad, R. (2018), "Energy-based evaluation of liquefaction of fiber-reinforced sand using cyclic triaxial testing", *Soil Dyn. Earthq. Eng.*, **104**, 45-53. https://doi.org/10.1016/j.soildyn.2017.09.026.

Ashmawy, A.K. and Bourrdeau, P.L. (1998), "Effect of geotextile reinforcement on the stress- strain and volumetric response of sand", *Proceedings of the 6th International Conference on Geosynthetics*, Atlanta, Georgia, U.S.A., March.

Baziar, M.H. and Jafarian, Y. (2007), "Assessment of liquefaction triggering using strain energy concept and ANN model capacity energy" *Soil Dyn. Earthq. Eng.*, **27**(12), 1056-1072. https://doi.org/10.1016/j.soildyn.2007.03.007.

Baziar, M.H., Jafarian, Y., Shahnazari, H., Movahed, V. and Tutunchian, M.A. (2011), "Prediction of strain energy-based liquefaction resistance of sand-silt mixtures: An evolutionary approach", *Comput. Geosci.*, **37**(11), 1883-1893. https://doi.org/10.1016/j.cageo.2011.04.008.

Cavallaro, A., Capilleri, P. and Grasso, S. (2018), "Site characterization by in situ and laboratory tests for liquefaction potential evaluation during Emilia Romagna earthquake", *Geosciences*, **8**(7), 1-15. https://doi.org/10.3390/geosciences8070242.

Chegenizadeh, A., Keramatikerman, M. and Nikraz, H. (2018), "Liquefaction resistance of fibre reinforced low-plasticity silt", *Soil. Dyn. Earthq. Eng.*, **104**, 372-377. https://doi.org/10.1016/j.soildyn.2017.11.004.

Chen, C.W. and Loehr, J.E. (2008), "Undrained and drained triaxial tests of fiber-reinforced sand", *Proceedings of the 4th Asian Regional Conference on Geosynthetics*, Shanghai, China.

Consoli, N.C., Montardo, J.P., Prietto, P.D.M. and Pasa, G.S. (2002), "Engineering behavior of a sand reinforced with plastic waste", *J. Geotech. Geoenviron. Eng.*, **128**(6), 462-472. https://doi.org/10.1061/(ASCE)1090-0241(2002)128:6(462).

Davis, R.O. and Berrill, J.B. (2001), "Pore pressure and dissipated energy in earthquakes-field verification", *J. Geotech. Geoenviron. Eng.*, **127**(3), 269-274. https://doi.org/10.1061/(ASCE)1090-0241(2001)127:3(269).

DeAlba, P., Seed, H.B. and Chan, C.K. (1976), "Sand liquefaction in large-scale simple shear tests", *J. Geotech. Eng. Div.*, **102**(GT9), 909-927

Diambra, A., Ibraim, E., Muir Wood, D. and Russell, A.R. (2010), "Fibre reinforced sands: Experiments and modelling", *Geotext. Geomembr.*, **28**(3), 238-250. https://doi.org/10.1016/j.geotexmem.2009.09.010.

Diambra, A., Russell, R., Ibraim, E. and Wood, D. (2007), "Determination of fibre orientation distribution in reinforced sand", *Geotechnique,* **57**(7), 623-628. https://doi.org/10.1680/geot.2007.57.7.623.

Erken, A., Torabi, M., Sargın, S. and Darvishi, A. (2015), "Liquefaction resistance of reinforced sands", *Proceedings of the 6th International Geotechnical Symposium on Disaster Mitigation in Special Geoenvironmental Conditions*, Chennai, India, January.

Figueroa, J., Saada, A., Liang, L. and Dahisaria, N. (1994), "Evaluation of soil liquefaction by energy principles", *J. Geotech. Eng.*, **120**(9), 1554-1569. https://doi.org/10.1061/(ASCE)0733-9410(1994)120:9(1554).

Fioravante, V., Giretti, D., Abate, G., Aversa, S., Boldini, D., Capilleri, P. P., Cavallaro, A., Chamlagain, D., Crespellani, T., Dezi, F., Facciorusso, J., Ghinelli, A., Grass,o S., Lanzo, G., Madiai, C., Massimino, M. R., Maugeri, M., Pagliaroli, A., Ranieri, C., Tropeano, G., Santucci De Magistris, F., Sica, S., Silvestri, F. and Vannucchi, G. (2013), "Earthquake geotechnical engineering aspects: The 2012 Emilia Romagna Earthquake (Italy)", *Proceedings of the 7th International Conference on Case Histories in Geotechnical Engineering*, Wheeling, Chicago, U.S.A., April-May.

Ghazavi, M. and Roustaei, M. (2010), "The influence of freeze-thaw cycles on the unconfined compressive strength of fiber-reinforced clay", *Cold Reg. Sci. Technol.*, **61**(2-3), 125-131. https://doi.org/10.1016/j.coldregions.2009.12.005.

Göktepe, B.A., Altun, S. and Lav, A.M. (2008), "Liquefaction resistance of sand reinforced with geosynthetics", *Geosynth. Int.*, **15**(5), 322-332. https://doi.org/10.1680/gein.2008.15.5.322.

Green, R.A. (2001), "Energy-based evaluation and remediation of liquefiable soils", Ph.D. Dissertation, Virginia Polytechnic Institute and State University, Blacksburg, Virginia, U.S.A.

Gullu, H. and Khudir, A. (2014), "Effect of freeze-thaw cycles on unconfined compressive strength of fine-grained soil treated with jute fiber, steel fiber and lime", *Cold Reg. Sci. Technol.*, **106-107**, 55-65. https://doi.org/10.1016/j.coldregions.2014.06.008.

Hejazi, S.M., Sheikhzadeh, M., Abtahi, S.M. and Zadhoush, A.A. (2012), "Simple review of soil reinforcement by using natural and synthetic fibers", *Constr. Build Mater.*, **30**, 100-116. https://doi.org/10.1016/j.conbuildmat.2011.11.045.

Ibraim, E., Diambra, A., Muir Wood, D. and Russell, A.R. (2010), "Static liquefaction of fibre reinforced sand under monotonic loading", *Geotext. Geomembr.*, **28**(4), 374-385. https://doi.org/10.1016/j.geotexmem.2009.12.001.

Ishihara, K. (1985), "Stability of natural deposits during earthquakes", *Proceedings of the 11th International Conference on. Soil Mechanics and Foundation Engineering*, San Francisco, California, U.S.A., August.

Ishihara, K. (1993), "Liquefaction and flow failure during earthquakes", *Geotechnique*, **43**(3), 351-415. https://doi.org/10.1680/geot.1993.43.3.351.

Jafarian, Y., Towhata, I., Baziar M.H., Noorzad A. and Bahmanpour, A. (2012), "Strain energy-based evaluation of

liquefaction and residual pore water pressure in sands using cyclic torsional shear experiments", *Soil Dyn. Earthq. Eng.*, **35**, 13-28. https://doi.org/10.1016/j.soildyn.2011.11.006.
Jones, M. (1999), *Mechanics of Composite Materials*, Taylor and Francis, Philadelphia, Pennsylvania, U.S.A.
Keramatikerman, M., Chegenizadeh, A. and Nikraz, H. (2017), "Experimental study on effect of fly ash on liquefaction resistance of sand", *Soil Dyn. Earthq. Eng.*, **93**, 1-6. https://doi.org/10.1016/j.soildyn.2016.11.012.
Kokusho, T. (2013), "Liquefaction potential evaluations: Energy-based method versus stress-based method", *Can. Geotech. J.*, **50**(10), 1-12. https://doi.org/10.1139/cgj-2012-0456.
Komak Panah, A., Yazdi, M. and Ghalandarzadeh, A. (2015), "Shaking table tests on soil retaining walls reinforced by polymeric strips", *Geotext. Geomembr.*, **43**(2), 148-161. https://doi.org/10.1016/j.geotexmem.2015.01.001.
Krishnaswamy, N.R. and Isaac, N.T. (1994), "Liquefaction potential of reinforced sand", *Geotext. Geomembr.*, **13**(1), 23-41. https://doi.org/10.1016/0266-1144(94)90055-8.
Krishnaswamy, N.R. and Isaac, N.T. (1995), "Liquefaction analysis of saturated reinforced granular soils", *J. Geotech. Eng.*, **121**(9), 645-651. https://doi.org/10.1061/(ASCE)0733-9410(1995)121:9(645).
Ladd, R.S. (1978), "Preparing test specimens using under compaction", *Geotech. Test. J.*, **1**(1), 16-23. https://doi.org/10.1520/GTJ10364J.
Law, K.T., Cao, Y.L. and He, G.N. (1990), "An energy approach for assessing seismic liquefaction potential", *Can. Geotech. J.*, **27**(3), 20-29. https://doi.org/10.1139/t90-043.
Liang, L. (1995), "Development of an energy method for evaluating the liquefaction potential of a soil deposit", Ph.D. Dissertation, Case Western Reserve University, Cleveland, Ohio, U.S.A.
Lovisa, J., Shukla, S.K. and Sivakugan, N. (2010), "Shear strength of randomly distributed moist fibre-reinforced sand", *Geosynth. Int.*, **17**(2), 100-106.
Maheshwari, B.K., Singh, H.P. and Saran, S. (2012), "Effects of reinforcement on liquefaction resistance of Solani sand", *J., Geotech. Geoenviron. Eng.*, **138**(7), 831-840. https://doi.org/10.1061/(ASCE)GT.1943-5606.0000645.
Monkul, M.M., Gultekin, C., Gulver, M., Akin, O. and Bayat, E.E. (2015), "Estimation of liquefaction potential from dry and saturated sandy soils under drained constant volume cyclic simple shear loading", *Soil Dyn. Earthq. Eng.*, **75**, 27-36. https://doi.org/10.1016/j.soildyn.2015.03.019.
Nemat-Nasser S. and Shokooh A. (1979), "A unified approach to densification and liquefaction of cohesionless sand in cyclic shearing", *Can. Geotech. J.*, **16**(4), 659-678. https://doi.org/10.1139/t79-076.
Noorzad, R. and Fardad, A.P. (2014), "Liquefaction resistance of Babolsar sand reinforced with randomly distributed fibers under cyclic loading", *Soil Dyn. Earthq. Eng.*, **66**, 281-292. https://doi.org/10.1016/j.soildyn.2014.07.011.
Noorzad, R. and Omidvar, M. (2010), "Seismic displacement analysis of embankment dams with reinforced cohesive shell", *Soil Dyn. Earthq. Eng.*, **30**(11), 1149-1157. https://doi.org/10.1016/j.soildyn.2010.04.023.
Orakoglu, M.E., Liu, J. and Niu, F. (2017), "Dynamic behavior of fiber-reinforced soil under freeze-thaw cycles", *Soil Dyn. Earthq. Eng.*, **101**, 269-284. https://doi.org/10.1016/j.soildyn.2017.07.022.
Ostadan, F., Deng, N. and Arango, I. (1996), "Energy-based method for liquefaction potential evaluation", Phase I. feasibility study, U.S. Department of Commerce, Technology Administration, National Institute of Standards and Technology, Building and Fire Research Laboratory, Gaithersburg, Maryland, U.S.A.
Park, S. (2011), "Unconfined compressive strength and ductility of fiber-reinforced cemented sand", *Constr. Build. Mater.*, **25**, 1134-1138. https://doi.org/10.1016/j.conbuildmat.2010.07.017.
Pincus, H.J., Maher, M.H. and Ho, Y.C. (1993), "Behavior of fiber reinforced cemented sand under static and cyclic loads", *Geotech. Test. J.*, **16**(3), 330-338. https://doi.org/10.1520/GTJ10054J.
Sadek, S, Najjar, S.S. and Freiha, F. (2010), "Shear Strength of fiber reinforced sands", *J. Geotech. Geoenviron. Eng.*, **136**(3), 490-499. https://doi.org/10.1061/(ASCE)GT.1943-5606.0000235.
Sharma, V. and Kumar, A. (2017), "Influence of relative density of soil on performance of macro-synthetic and non-corrosive fiber-reinforced soil foundations", *Geotext. Geomembr.*, **45**(5), 499-507. https://doi.org/10.1016/j.geotexmem.2017.06.004.
Simcock, J. Davis, R.O. Berrill, J.B. and Mallenger, G. (1983), "Cyclic triaxial tests with continuous measurement of dissipated energy", *Geotech. Test. J.*, **6**(1), 35-39. https://doi.org/10.1520/GTJ10822J.
Sonmezer, Y.B. (2019), "Energy-based evaluation of liquefaction potential of uniform sands", *Geomech. Eng.*, **17**(2), 145-156. https://doi.org/10.12989/gae.2019.17.2.145.
Tang, C.S., Wang, D.Y., Shi, B. and Li, J. (2016), "Effect of wetting-drying cycles on profile mechanical behavior of soils with different initial conditions", *Catena*, **139**, 105-116. https://doi.org/10.1016/j.catena.2015.12.015.
Towhata, I. (2008), *Geotechnical Earthquake Engineering*, Springer-Verlag, Berlin Heidelberg.
Towhata, I. and Ishihara, K. (1985), "Shear work and pore water pressure in untrained shear", *Soils Found.*, **25**(3), 73-84. https://doi.org/10.3208/sandf1972.25.3_73.
Vercueil, D., Billet, P. and Cordary, D. (1997), "Study of the liquefaction resistance of a saturated sand reinforced with geosynthetics", *Soil Dyn. Earthq. Eng.*, **16**(7-8), 417-425. https://doi.org/10.1016/S0267-7261(97)00018-3.
Wang, S., Luna, R. and Stephenson, R.W. (2011), "A slurry consolidation approach to reconstitute low-plasticity silt specimens for laboratory triaxial testing", *Geotech. Test. J.*, **34**(4), 1-9. https://doi.org/10.1520/GTJ103529.
Ye, B., Cheng, Z.R., Liu, C., Zhang, Y.D. and Lu, P. (2017), "Liquefaction resistance of sand reinforced with randomly distributed polypropylene fibres", *Geosynth. Int.*, **24**, 626-636. https://doi.org/10.1680/jgein.17.00029.
Zaimoglu, A.S. (2010), "Freezing-thawing behavior of fine-grained soils reinforced with polypropylene fibers", *Cold Reg. Sci. Technol.*, **60**(1), 63-65. https://doi.org/10.1016/j.coldregions.2009.07.001.

CC